

# Concentrated Load on Top of Geosynthetic-Reinforced Earth Structures

P. Villard, Ph. Gotteland & J. -P. Gourc  
IRIGM, University Joseph Fourier, Grenoble, France

Y. Matichard  
GeoSyntec Consultants, Boca Raton, FL, USA

**ABSTRACT :** The recent applications of reinforced earth structures to support other structural works (e.g. bridge abutment) led to the construction of full scale test structures, which were subjected to concentrated loads on top up to failure. In this paper, numerical models (finite element and limit equilibrium methods) are presented. The aim of the numerical modelling was mainly to understand and to anticipate the failure mechanisms of an instrumented full scale test wall.

## 1 INTRODUCTION

An European co-operation based on the wish to increase the application possibilities of reinforced earth structures, was established between the BAST in Germany and the LCPC in France, and a test programme was carried out related to the design of reinforced structure, subjected to loads applied on top (Balzer and al, 1990). The experimental part concerned an instrumented full scale test wall, which was constructed at the BAST in Germany according to the French process Ebal-LCPC (Gourc and al, 1994). The numerical modelling of the test presented in this paper, was performed in the IRIGM-L.g.m at Grenoble. A large displacements finite element analysis considering the great deformations induced during serviceability was adopted. A limit equilibrium analysis is further presented to validate a design method for the prediction of the failure load.

## 2 MEASUREMENT RESULTS

The instrumented structure, basis reference of the numerical modelling was a 2.88 m high by 3.93 m wide and 3.75 m long (lateral) full scale test wall. The test wall had five geotextile sheets and five granular soil layers each 0.5 m in height. The total length of the geotextile sheets was 3.5 m, consisting of 1 m effective length for the underlap, 0.5 m thickness for the facing and 2 m effective length for the upper reinforcement. The test wall was loaded on top by a loading frame which produces

vertical loads  $P$  on a rigid concrete slab with the dimensions : length - 2.40 m, width - 0.9 m. The full scale test wall was loaded stepwise up to failure (Fig. 1).

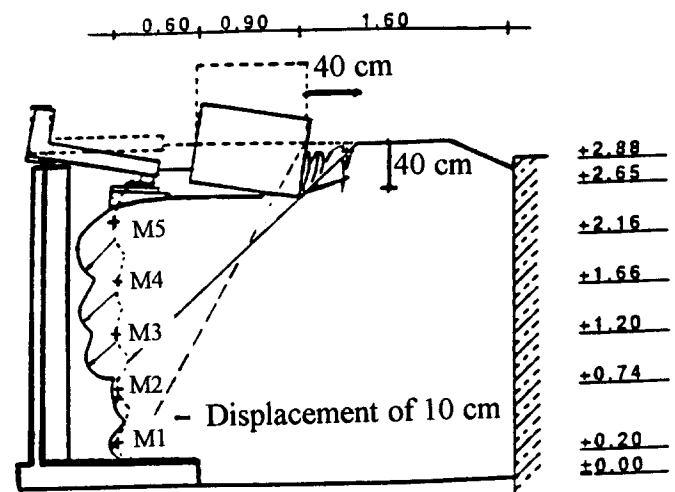


Fig. 1 Displacements within the test wall after failure

The 2.9 mm thick geotextile used, was a needle-punched nonwoven made from polyester fibres. A stiffness  $J$  of 48,6 kN/m and a tensile strength at failure  $T_f$  of 18 kN/m were obtained from tensile tests on a 500 mm wide and 100 mm long geotextile sample.

The coarse grained fill material was a gravely sand from locations of the Rhine valley with a unit weight of 19.8 kN/m<sup>3</sup>. The cohesion and the angle of internal friction which were determined with reconstructed and

compacted soil sample in a shear box, were respectively 8 kPa and 37°. Friction tests on the materials gave Mohr Coulomb frictional behaviours with friction values of 31.5° and 16° respectively for the interfaces soil-geotextile and geotextile-geotextile.

Numerous measurements were performed to monitor displacements of the wall facing, settlements of the loading slab, strains on the reinforcements and stresses within the fill. Arrangements reducing bound frictional effects, the high lateral length of the loading slab and the measurements taken in the middle axis of the test wall, allowed to performed analysis in plane strain. Measurement results (Fig. 2) and observations during loading have shown the development of two successive failure modes of the structure up to collapse.

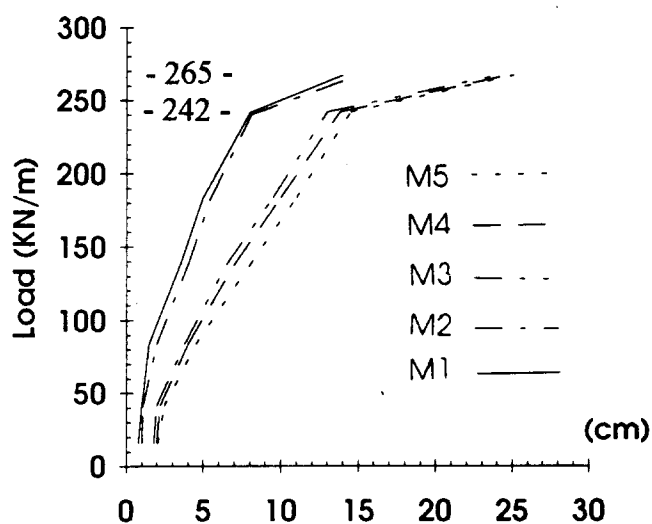


Fig. 2 Measured displacements of the Mi-locations on the facing

The first failure mode was similar to an overturning of the structure up to a load of 242 kN/m with about 15 cm displacements reached on top. The yielded zone consist of a failure wedge going through the toe.

Cracks located about 40 cm behind the loading slab developed from a load of 242 kN/m. The second failure mode started thereafter up to a load of 265 kN/m until the total collapse of the test wall occurred along a slip surface. The collapse developed as successive failures of the upper reinforcements, sliding of the three upper earth layers over the lowers, rotation and puncture of the loading slab. The yielded zone was a failure wedge coming out at the toe of the third layer.

### 3 NUMERICAL MODELLING

#### 3.1 Finite Element Approach

The finite element method used was the large displacements analysis considering a second degree

relationship between displacements and strains (Gourc and al, 1992). The parametric study was based on an elastoplastic relationship for soil and an elastic one for the geotextile. The behaviour at the interfaces was non-linear. The used computer program (GOLIATH) has been developed at the IRIGM to investigate cases with large displacements at the interface.

#### 3.2 Validation of the finite Element Approach

The adopted 2D-mesh model (Fig. 3) was composed of 1586 triangular elements, 125 bar elements and 1038 nodes. The boundary conditions were friction at the base of the structure and purely sliding at the backfill. The soil-geotextile interface was treated with a three-lined node element, one element representing the geotextile and the two others modelling the soil placed over and below the reinforcement. The bound was established by separation and forces equilibrium conditions.

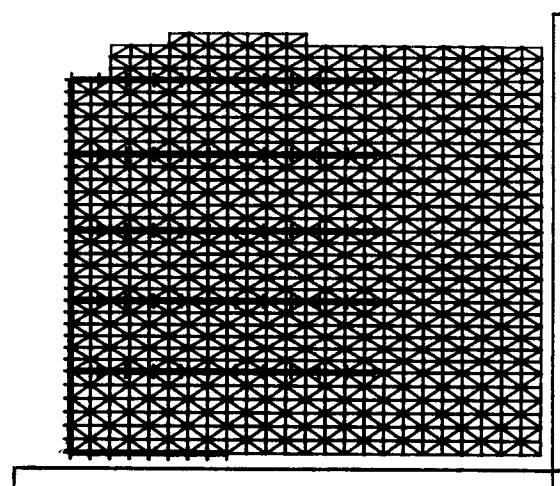


Fig. 3 Initial mesh of the test wall

The geotextile sheets were modelled by two-node bar elements which allowed the simulation of the membrane behaviour (no bending stiffness), and supposed to be elastic materials in tension (no compression). The soil was modelled as an elastic-perfectly plastic material ( $E = 50 \text{ MPa}$  et  $\nu = 0,33$ ) with associated load and flow surfaces. The Matsuoka and Nakai plasticity criterion (Matsuoka and nakai, 1982) was adopted together with the already mentioned parameters.

The initial behaviour of the structure before loading on top, was simulated by a successive loading represented the self weight. Therefore stages due to the construction procedure (Ebal-LCPC) such as fill densification, relaxation of soil beneath the facing (geotextile yielding) and the stretching of reinforcements, were not correctly modelled. The concrete slab transmitting loads from the loading frame was placed free on top.

The performed analysis up to failure are presented on Fig. 4 and 5.

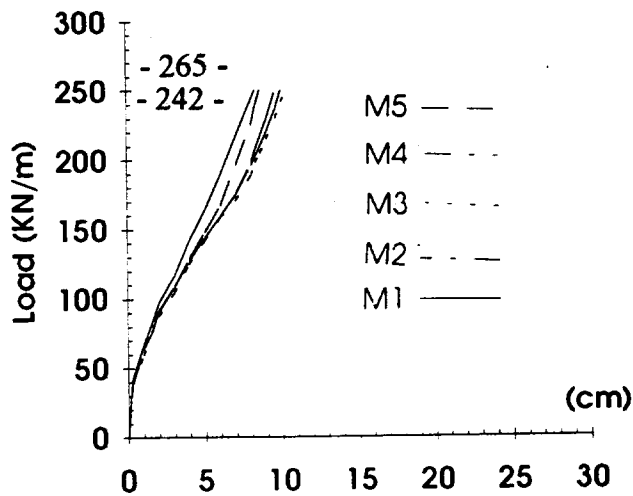


Fig. 4 Theoretical displacements of the  $M_i$ -locations on the facing

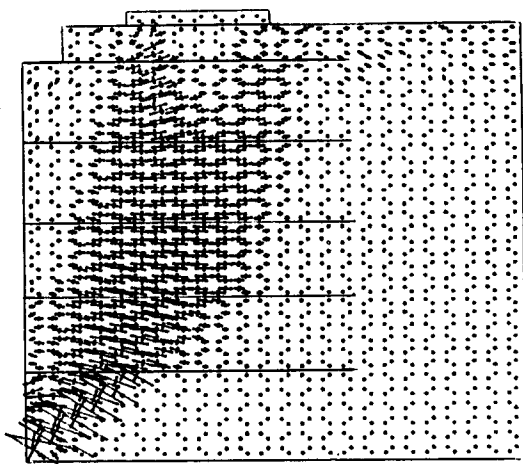


Fig. 5 Main strains within the structure for  $P=265$  kN/m

The displacement results of Fig. 4 show a correlation between theoretical and measured displacements for the first behaviour mode ( $P < 242$  kN/m). The second behaviour mode ( $P > 242$  kN/m) induced certainly by complex mechanisms, due to stresses concentrations within the fill, could not be modelled. The obtained strains (Fig. 5) for a load  $P$  of 265 kN/m have shown strong yielded zones and a stiff wedge below the loading slab.

The maximum tensile strength values obtained (6.9 kN/m) at a load  $P$  of 265 kN/m were much lower than those required for the failure of geotextile. Note that values calculated from maximum measured strains were all found less than 2 kN/m, even much higher local strengths could be expected. In fact, the concentrated loads on top induced higher vertical pressures below the loading slab for the upper reinforcements, so that great tensile gradients on the geotextile sheets occurred.

From the results, it can be seen that the structure didn't failed by reinforcements pullout. In fact, the vertical pressures applied on the geotextiles can provide important stresses concentration for a 20 cm anchorage

length, so that maximum tensile strengths could be mobilised within the reinforcements. In this case, a rupture of the geotextile occurred instead a pullout failure.

On the other hand, the soil should be deformed in shear since large deformations were observed within the fill (more than 15%). The use of more sophisticated relationship for the soil behaviour as well as adapted analysis algorithms may simulate the second failure mode of the structure.

## 4 LIMIT EQUILIBRIUM APPROACH

### 4.1 The two blocks method

This method consists of assuming the overall equilibrium of the active zone. It doesn't allow to satisfy the three equations of equilibrium for a bilinear line of slippage (equilibrium of moments is not satisfied).

Already presented (Gourc and al, 1988), the method has been adapted for the calculation of wall with local sollicitation. It should be observed that the force at the interface is perpendicular to the line between the two blocks.

For the mobilization of tensile forces in the reinforcements it is assumed that the available tensile forces are :

$$T_j \text{ available} = \min (T_f/f_f, T_{pj\max}/f_p)$$

$T_f$  is the ultimate tensile force at failure ( $f_f$  factory safety) and  $T_{pj\max}$  is the maximum pull-out anchoring force ( $f_p$  Factor of safety)

It is now possible to inclinate the tension (inclination  $\beta_j$ ) to take into account the local conditions of relative soil-geotextile rigidity. In the present case  $\beta_j=0$ .

The equation of equilibrium yield FS, the factor of safety on shear of the soil along the slip line.

### 4.2 Validation of the two-blocks method

We consider that there is rupture for factor of safety  $FS=1$  along potential lines of rupture (bilinear lines having a geometry passing through the zones of maximal displacement gradient in the experimentation results (line 1 and line 2 Fig. 6) . By contrast with the usual structural design approach, we assume no reduction of the maximum pull-out anchoring forces ( $f_f=1, f_p=1$ ).

We will distinguish two cinematics corresponding to the two observed phases. The first one, until  $P=242$  kN/m, with a linear slip line passing through the base of the wall (line 1). The second one, after  $P=242$  kN/m, with a bilinear slip line with slipping on the geotextile at the base of the third layer of soil (line 2).

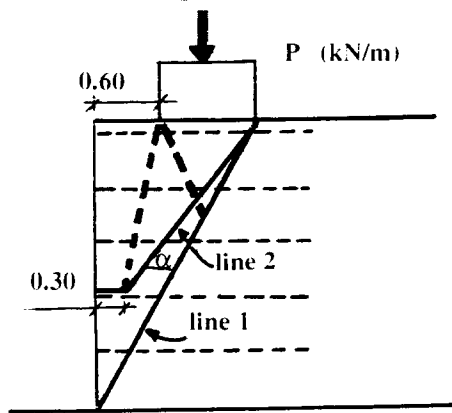


Fig. 6 Two Blocks Method : Mechanisms used for calculation during the two phases

The limit equilibrium calculation allow us to obtain the sum of the tensile forces to mobilize  $n.T$  ; with  $n$  number of sheets intersected by the slip line. Then, we calculate the tensile force  $T_j$  in each geotextile sheet (in this case, the pull-out anchoring force is always satisfied :  $T_j=T$ ).

Fig.7 shows the evolution of the tensile force  $T$  during various stages. In the first part of the experiment (line 1, calculation 1) we have an increasing of the mobilized tensile forces with the increasing surcharge  $P$ . A degree of compatibility with the experiment can be seen : we obtain tensile force  $T > T_f = 18\text{kN/m}$  for  $P=242\text{ kN/m}$  corresponding to the limit between phase 1 and phase 2 (Fig. 2).

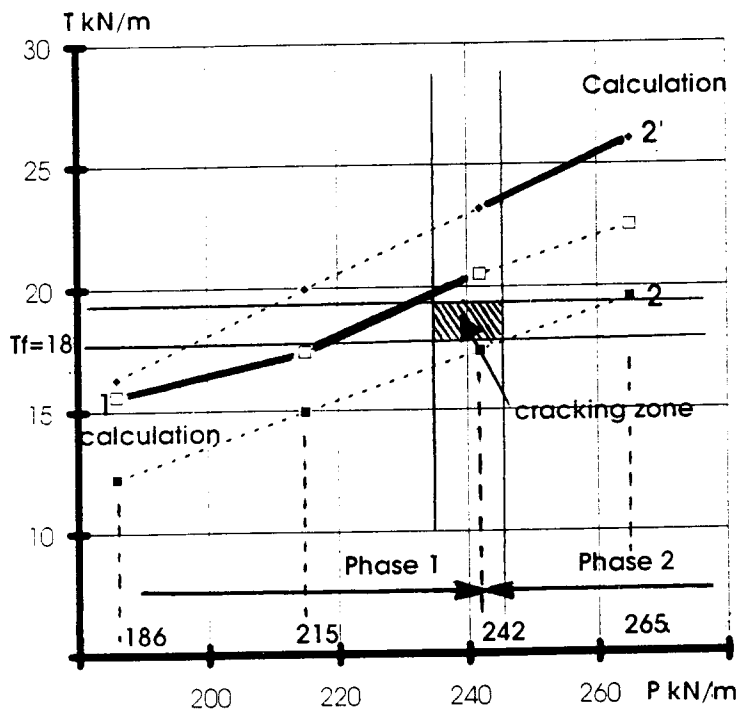


Fig. 7 Evolution of tensile force  $T$  with  $P$  different assumptions for the calculation

In the second phase of the experiment the failure is localized at the top of the wall (Fig. 1) ; the calculation is made on line 2 (calculation 2 and 2' Fig. 7) for  $P=242$

$\text{kN/m}$  and  $P=265\text{ kN/m}$ . It should be possible to assign the exchange of the first mechanism (line 1) for the second one (line 2) at the cracking of one sheet of geotextile in the upper part of the wall; this last point justify the calculation 2'. The cracking zone (Fig. 7) corresponds to the range of dubiouness on the maximal strength of the geotextile in confine state and on the surcharge  $P$  inducing the geotextile failure.

Because of the value  $T > T_f$  and of the observed cinematic, we are now able to justify the hypothesis of one inclination of the tensile forces ( $\beta_j=0$ ), wich involve their diminution. Indeed, the low stiffness of the geotextile let us think that experimental inclinations of the tensile  $\beta_j$  could be  $\beta_j = \alpha$  in the upper part of the wall. It will be the subject of an other paper wich will be presented otherwise.

## 5 CONCLUSION

Although the numerical analysis show interesting results, particularly for the first behaviour mode and gave satisfied descriptions of the failure mode, it seems necessary to proceed with modelling for the determination of strains within the structure and for the prediction of the failure load.

## REFERENCES

- Balzer, E. and Delmas, P. and Matichard, Y. and Sere, A. and Thamm B.R. (1990) Performance of reinforced soil structures, *British Geotechnical Society*, 47-52.
- Gourc, J.P. and Matichard, Y. (1994) Two decades of geosynthetic-reinforced retaining structures in France, *Proceedings of Seiken Symposium*, "Recent case histories of permanent geosynthetic reinforced soil reteneing wall", N°11, Tokyo, Japan, Balkema.
- Gourc, J.P. and Villard, P. and Matichard, Y. (1992) Pull-out behaviour of reinforcements Centrifuge tests and theoretical validations, *International Symposium on Earth Reinforcement Practice*, Kyushu, Japan.
- Matsuoka, H. and Nakai T. (1982) A new failure criterion for soils in three-dimensional stresses, *Conference on Deformation and Failure of Granular Materials*, I.U.T.A.M., Delft, 253-263.

- Gourc, J.P. and Ratel, A. and Gotteland, Ph. (1988) Design of reinforced soil retaining walls. Analysis and comparison of existing design method and proposal for a new approach, *The applications of polymeric reinforcement in soil retaining structures*, Nato ASI Series, Applied Sciences, Vol 147, 459-506.